Boundary estimation in electrical impedance tomography with multi-layer neural networks

Jae-Hyoung. Kim*, Hae-Jin Jeon*, Bong-Yeol Choi*, Seung-Ha Lee*, Min-Chan Kim**, Sin Kim***, and Kyung Youn Kim****

* Department of Electronic Engineering, Kyungpook National University, Taegu, 702-701, Korea
(Tel: +82-53-940-8653; Fax: +82-53-9597336; Email: cjsrkd97@hanmail.net)
** Department of Chemical Engineering, Cheju National University, Cheju, 690-756, Korea
*** Department of Nuclear & Energy Engineering, Cheju National University, Cheju, 690-756, Korea
**** Department of Electrical and Electronic Engineering, Cheju National University, Cheju, 690-756, Korea
(Tel: +82-64-754-3664; Fax: +82-64-756-1745; Email: kyungyk@cheju.ac.kr)

Abstract: This work presents a boundary estimation approach in electrical impedance imaging for binary-mixture fields based on a parallel structured multi-layer neural network. The interfacial boundaries are expressed with the truncated Fourier series and the unknown Fourier coefficients are estimated with the parallel structure of multi-layer neural network. Results from numerical experiments shows that the proposed approach is insensitive to the measurement noise and has a strong possibility in the visualization of binary mixtures for a real time monitoring.

Keywords: Boundary estimation, electrical impedance tomography, the parallel structured multi-layer neural network, FEM

1. INTRODUCTION.

Electrical impedance tomography (EIT) is a relatively new imaging modality to reconstruct the distribution of electrical properties in the cross-section of the domain of interest. EIT has obvious potentials for the imaging or monitoring in many areas including medical and process engineering applications due to its noninvasive characteristic, good temporal resolution and low-cost requirements. In this work, we intend to apply EIT to the visualization of binary-mixture fields, which may be commonly encountered under normal as well as accidental conditions in two-phase flows in many heat transfer systems and two-component flows in various industrial processes. Knowledge on the mixture distribution of such flows is of importance for the design and the safety analysis.

There have been many attempts from both theoretical and experimental points of view for the visualization of binary mixtures. According to their physical bases, radiological, optical, sonic, magnetic, and electrical properties are used to reconstruct the mixture distribution or to monitor the behavior of mixture flow. Various industrial tomography techniques from basic ideas to their applications could be found in [1]. Especially, applications of electrical tomography for binary mixtures are well reviewed in [2].

For this purpose, the present work adopts EIT, where an array of disjoint electrodes is placed on the boundary of object and a set of the predetermined electrical currents is imposed through the electrodes, and then the corresponding set of electrical potentials is measured at the electrodes. The objective is to estimate the conductivity distribution inside the problem domain based on the relation between the imposed currents and the measured voltages. The image reconstruction of EIT is considered as an optimization problem, which is composed of the forward problem calculating the boundary potentials with the assumed conductivity distribution and the inverse problem updating the conductivity distribution to reduce the difference between the measured and the calculated boundary voltages. Hence, the forward and the inverse solvers are alternately applied as usual until the convergence.

The procedure for the solution of EIT inverse problem seems to be quite straightforward; however the ill-posed nature of the problem tends to impede the convergence and fine spatial resolution. In order to improve the convergence characteristic, the regularization based on prior information is often introduced successfully, whereas regularization may sacrifice the spatial resolution for the convergence. Hence, the improvement of convergence characteristics and the enhancement of spatial resolution are an issue of importance.

Especially for binary mixtures, the mesh-grouping method, the mesh-refinement method and simple multi-layer neural network method would be noteworthy. The first can reduce the number of unknowns significantly and can consequently enhance the sensitivity of the change on the boundary voltages to the change of conductivity distribution [3, 4]. In the second, the algorithm adapts to the reconstructed object boundary by generating finer meshes in areas where there are sharp gradients in the images based on an *a posteriori* error estimate [5]. In the last, the algorithm adapts to the reconstructed object boundary by single multi-layer neural network based on change of boundary voltage to the change of conductivity distribution [8].

Some investigators have focused on the reconstruction of mixture interface rather than mixture distribution in the EIT image reconstruction. If the conductivity value of each component in mixtures could be given *a priori*, the unknown would be the interfacial boundary. Han and Prosperetti [6] considered a shape decomposition technique based on the boundary element method, where the boundary of each object was represented in terms of Fourier coefficients rather than a point-wise discretization. Kolehmainen *et al.* [7] developed an algorithm to recover the region boundaries of piecewise constant coefficients of an elliptic PDE from boundary data for the application to optical tomography, which will of course be applicable to EIT. They also expressed boundaries in terms of Fourier coefficients. For the optimal solution of the Fourier coefficients, they employed Newton-type method, which is usually time consumed although it has shown a good

performance in many optimization problems. Such slow convergence would be an adverse effect in the application to mixture flows undergoing fast transient.

This paper presents a novel approach to estimate the boundary of each object with the parallel structured multi-layer neural network (PMNN) since PMNN has advantages in its conceptual simplicity, robustness of environment of target, ease of implementation, and the ability to control the compromise between the noise treatment and the spatial resolution.

As formulated in [6-7], we approximate the boundary as the truncated Fourier series, whose coefficients will be estimated with the aid of PMNN. In the PMNN approach, the solution procedure is composed of four stages. First, each multi-layer neural network trains weighting matrices for using a series of forward problems and their solutions until the weighting matrices 'figure out' the problem-solving technique. That is, we need a training set, consisting of voltage measurements and the object boundaries that produce the boundary voltages. This training set should be produced experimentally, but it would be overly time consuming to obtain the necessary size of training set. In this paper, hence, we use a finite element model of the problem domain to generate the training set numerically by solving the forward problem. In the second stage, the weighting matrices constructed with using the training set are incorporated in the inverse solution to estimate the unknown Fourier coefficients in each multi-layer neural network from the measured boundary voltage data. In the third stage, we calculate the boundary voltage using estimated each Fourier coefficient and finite element method. In the fourth stage, we define the weighting from root mean square of boundary voltage. The numerical experiments are successfully carried out to illustrate the performance of the proposed approach.

2. THE MATHEMATICAL MODEL

2.1. Forward Problem

The forward problem is to compute the electrical potential when the injected current and the conductivity distribution are given. When electrical currents $I_l (l = 1,2,\cdots,L)$ are injected into the object $\Omega \in R^2$ through the electrodes $e_l (l = 1,2,\cdots,L)$ attached on the boundary $\partial\Omega$ and the conductivity distribution $\sigma(x,y)$ is known over the Ω, the corresponding induced electrical potential $u(x,y)$ can be determined uniquely from following partial differential equation, which can be derived from the Maxwell equations:

$$\nabla \cdot (\sigma \nabla u) = 0, \qquad \text{in } \Omega \tag{1}$$

The boundary conditions in the complete electrode model are given as:

$$\left(u + z_l \sigma \frac{\partial u}{\partial n} \right)\Big|_{e_l} = U_l, \quad l = 1,2,\cdots,L \tag{2}$$

$$\int_{e_l} \sigma \frac{\partial u}{\partial n} dS = I_l, \qquad l = 1,2,\cdots,L \tag{3}$$

$$\sigma \frac{\partial u}{\partial n}\Big|_{\partial\Omega \setminus \bigcup_{l=1}^{L} e_l} = 0 \tag{4}$$

where z_l is the effective contact impedance between the ℓ-th electrode and the mixture field, U_l is the measured potential on the ℓ-th electrode, e_l is l-th electrode, n is the outward unit normal, and L is the number of electrodes. The boundary conditions (2)~(4) take into account the shunting effect (i.e. the voltage U_l is constant over the electrode e_l) and the additional voltage drop due to the contact impedance.

In addition, the following two conditions for the injected currents and the measured voltages are needed to ensure the existence and uniqueness of the solution:

$$\sum_{l=1}^{L} I_l = 0, \quad \sum_{l=1}^{L} U_l = 0 \tag{5}$$

In general, the forward problem cannot be solved analytically. So, we have to resort to the numerical method. In this paper, the finite element method (FEM) is used to obtain the numerical solution. In the FEM, the problem domain is discretized into sufficiently small elements having a node at each corner. And it is assumed that the conductivity distribution is constant within each element. The potential at each node and the "referenced" electrode voltage, defined by the vector $v \in R^{(M+L-1)\times 1}$, are calculated by discretizing (1) into $Yv = c$, where $Y \in R^{(M+L-1)\times(M+L-1)}$ is so called stiffness matrix and M is the number of FEM nodes, Y and c are the functions of the conductivity distribution inside the object and the injected currents through the electrodes, respectively. For more details on the forward solution and the FEM approach, see [9].

2.2. Boundary Expression and FEM Discretization

We assume that the outer boundaries of objects are sufficiently smooth and they can be approximated in the form

$$C_\ell(s) = \begin{pmatrix} x \\ y \end{pmatrix} = \sum_{n=1}^{N_\theta} \begin{pmatrix} \gamma_n^{x_\ell} \theta_n^x(s) \\ \gamma_n^{y_\ell} \theta_n^y(s) \end{pmatrix} \tag{6}$$

as was in [6] and [7]. In (6), $C_\ell(s)$, $\ell = 1,\cdots,m$ is the boundary of the ℓ-th object, m is the number of the objects, $\theta_n(s)$ is a periodic and differentiable basis function with period 1, and N_θ is the number of basis functions. As the basis function, we use the form of

$$\begin{aligned} &\theta_1^\beta(s) = 1 \\ &\theta_n^\beta(s) = \sin\left(2\pi \frac{n}{2} s\right), && n = 2,4,6,\cdots,even \\ &\theta_n^\beta(s) = \cos\left(2\pi \frac{(n-1)}{2} s\right), && n = 3,5,7,\cdots,odd \end{aligned} \tag{7}$$

where $s \in [0\ \ 1]$, β denotes either x or y. The boundaries of the objects are identified with the vector γ of

the shape coefficients.

$$\gamma = (\gamma_1^{x_1}, \cdots, \gamma_{N_\theta}^{x_1}, \gamma_1^{y_1}, \cdots, \gamma_{N_\theta}^{y_1}, \gamma_1^{x_m}, \cdots, \gamma_{N_\theta}^{x_m}, \gamma_1^{y_m}, \cdots, \gamma_{N_\theta}^{y_m})^T \quad (8)$$

where $\gamma \in R^{2mN_\theta}$.

The relation of the measured voltages on the electrodes and the Fourier coefficients γ defined above are very nonlinear. However, it should be clarified and then incorporated into the forward solver. Now, let's express the discretization of the forward model as a mapping from the Fourier coefficients γ to the boundary data of the injected currents and the measure potential. The spatial discretization of the forward problem is made with FEM, so the relation will be described in the sense of finite element formulation. In boundary estimation problems, the object boundary may not fit to the mesh boundary. Hence, the mesh should be reformed to adapt to the object boundary or the elements crossing the object boundary should be treated in a proper manner. This paper does not consider a re-meshing scheme. Including the treatment of boundary-crossing elements, the FEM implementation of this mapping can be accomplished in 4 stages as follows [7]:

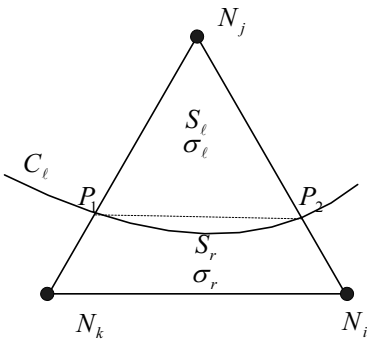

Fig. 1 Schematic of the finite element mesh crossing the object boundary $C_\ell(s)$.

Step1: Classify mesh nodes into inside or outside for a given boundary $C_\ell(s)$.

Step2: Classify the finite elements as inside, outside, or intercepted by the given boundary $C_\ell(s)$.

Step 3: Determine intersections of element edges, $C_\ell(P_1)$ and $C_\ell(P_2)$, with the given boundary $C_\ell(s)$, see Fig.1.

Step 4: Compute the system matrices. In this step, we approximate the boundary C_ℓ with a straight line from the intersection point $C_\ell(P_1)$ to the point $C_\ell(P_2)$, and then split the intercepted element into two parts. We approximate the effective conductivity of the intercepted element, σ_{cross}, as an area-averaged value

$$\sigma_{cross} = \frac{\sigma_\ell S_\ell + \sigma_r S_r}{S_\ell + S_r} \quad (9)$$

where σ_ℓ and σ_r are the conductivity of the object and the background, respectively. S_ℓ and S_r are the area that belongs to the object and the background, respectively.

Now, the shape coefficients γ are implicitly engaged in the finite element formulation through the area terms in (9).

2.2. Boundary estimation with the parallel structure of multi-layer neural network

In this work, we introduce the PMNN to reconstruct boundary shapes and locations of the targets. The PMNN has some advantages such as adaption characteristics to new situations and robustness against measurement noise. In the PMNN, the weighting matrices W_1^i, W_2^i of each MNN are trained using the relation of the change of the measured voltages f and the change of the Fourier coefficient $\Delta\gamma$ [8]. And the selection weighting We_i are defined by root mean squire of boundary voltage. The schematic diagram of MNN is shown in Fig. 2.

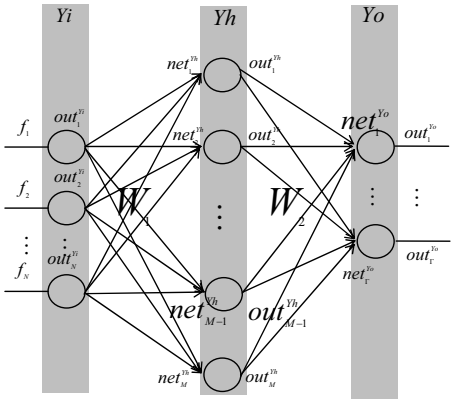

(a) Multi-layer neural network

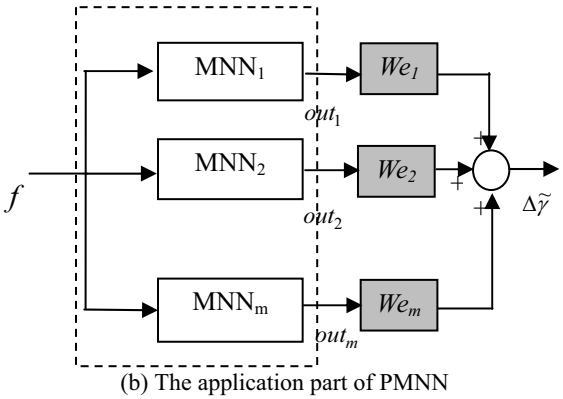

(b) The application part of PMNN

Fig. 2 Schematic diagram of the proposed PMNN.

To train the weighting matrices W_1^i, W_2^i $(i = 1, \cdots, m)$ of the PMNN, we use different sigmoid fuction g_i for each layer and the training set is composed of $\Delta\gamma$ and f. The sigmoid function g_i shows the non-linearity of the system

which is defined as

$$g_i(x) = \frac{\mu_i}{1 + e^{-l_i(x-c_i)}} + \lambda_i, \quad i = 1, \cdots, m \tag{10}$$

where $\mu_i, l_i, c_i, \lambda_i$ are parameters selected by the designer. The boundary voltage change f is defined as

$$f_n^k = \frac{v_n^k - v_n^{ref}}{v_n^k + v_n^{ref}} \quad \begin{matrix} k = 1, 2, \cdots, K \\ n = 1, 2, \cdots, N \end{matrix} \tag{11}$$

where v_n is the $n-th$ value of the measured boundary voltages for each frame, N is the number of boundary voltage data for a frame, K is the number of the learning data, and v^{ref} is the reference voltage. The change of the Fourier coefficients $\Delta\gamma$ is obtained as

$$\Delta\gamma_j^k = \frac{\gamma_j^k - \gamma_j^{ref}}{2} \quad \begin{matrix} k = 1, \cdots, K \\ j = 1, \cdots, 2mN_\theta \end{matrix} \tag{12}$$

The updating procedure for the weighting matrices W_1^i, W_2^i $(i = 1, \cdots, m)$ can be summarized by the following algorithm [8]:

Step 1: Initialize the weights W_1^i, $W_2^i (i = 1, \cdots, m)$ with small random numbers.

Step 2: Begin the training iteration.

Step 3: Calculate the outputs of each multi-layer neural network by

$$out_i = W_2^i \cdot g_i(W_1^i \cdot (f_n^k + 1_n^k)) + 1_n^k \tag{13}$$

Step 4: Calculate the error $e_i = \Delta\gamma - out_i$ and update each weights by the learning rule.

Step 5: Repeat from Step 2 to Step 4 until the stopping condition is satisfied.

After training, we can estimate m number of the Fourier coefficients out_i by using the change of the measured boundary voltages from the reference.

The determination of weighs matrices We_i can be summarized by the following algorithm:

Step 1: Calculate the boundary voltage V_{MNN_i} by using FEM and estimated Fourier coefficient out_i ($i = 1, \cdots, m$).

Step 2: Calculate the root mean square (RMSE) about each MNN

$$RMSE_i = \sqrt{\frac{(V_{mea} - V_{MNN_i})^T \cdot (V_{mea} - V_{MNN_i})^T}{V_{mea}^T \cdot V_{mea}}} \tag{14}$$

where V_{mea} are measured boundary voltage and V_{MNN_i} are boundary voltage by using FEM and estimated Fourier coefficient out_i.

Step 3: Find MNN_i with minimum value of $RMSE$ and define We_i

$$We_i = \begin{cases} 1 & \min(RMSE_i) \\ 0 & otherwise \end{cases} \tag{15}$$

The Fourier coefficient is obtained as

$$\Delta\hat{\gamma} = \sum_{i=1}^{m} WE_i \cdot out_i, \quad i = 1, \cdots, m \tag{16}$$

If the structure of PMNN is the parallel structure, although the off-line training procedure is computationally intensive and the structure is complex, the on-line calculation time taken to obtain (16) would be so fast, insensitive to the measurement noise and has a strong good possibility in the visualization of binary mixtures for a real time monitoring.

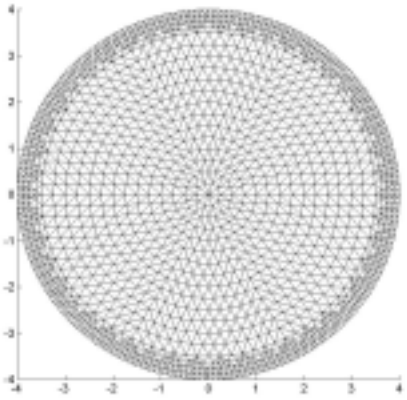

Fig. 3 FEM meshes used for forward problem.

3. NUMERICAL EXPERIMENTS

To show the effectiveness on our approach, numerical experiments have been carried out with a 32-channel EIT system. The problem domain is discretized into 3104 triangular elements with 1681 nodes in the context of FEM and the meshes are shown in Fig. 3. The resistivity values of the object and the background are set to 600Ωcm and 300Ωcm, respectively.

For the current injection, the opposite method is adopted and 512 boundary voltage inputs are used for a frame. The weighting matrices are trained with a training set with 2608 learning data (forward problems). The number of hidden layers is set to 48. The number of MNN is set to 4. We assume targets to be circular or elliptic, so the dimension of Fourier

series is set to $N_\theta = 3$.

In order to compare the performance of the proposed PMNN approach with that of the modified Newton-Raphson (mNR) methods [11-12], it is assumed that a single target with a various shape is placed at different location. Fig. 4 represents the reconstructed boundaries obtained from the surface voltage with 1% noise. As it can be seen, both approach the reveal similar reconstruction performance.

As the noise level increases, the reconstruction performance of the mNR is degraded significantly even though we started quite reasonable initial value. In particular, in Fig. 6(b) we can find the mNR converges to wrong location. On the other hand, the reconstructed boundaries obtained from the PMNN show comparatively good performance regardless of noise.

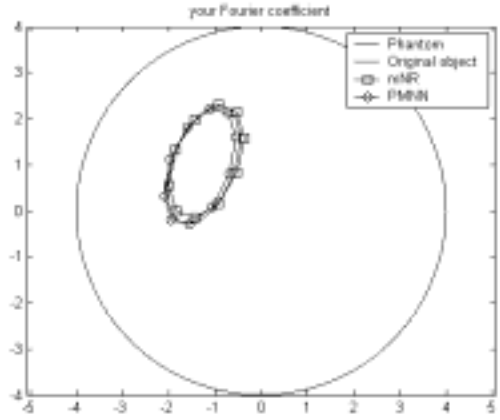

(a) γ = [-1.25, 0.75, 0.20, 1.00, 0.25, 1.25]

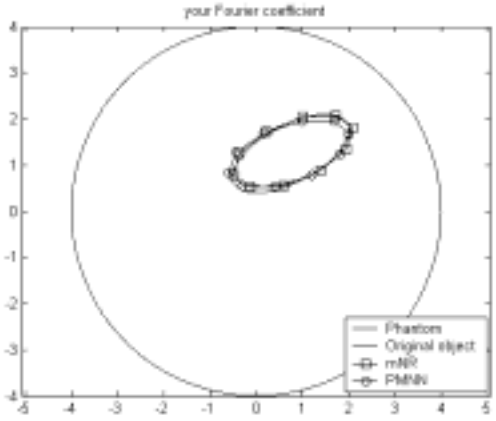

(b) γ = [0.75, 1.25, 0.20, 1.00 , 0.40, 0.75]

Fig. 4 Estimated boundary shape by PMNN and mNR with 1% noise

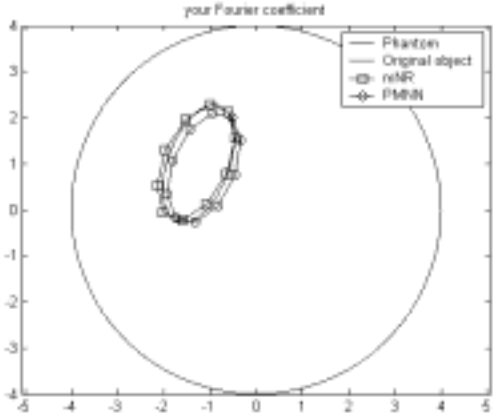

(a) γ = [-1.25, 0.75, 0.20, 1.00, 0.25, 1.25]

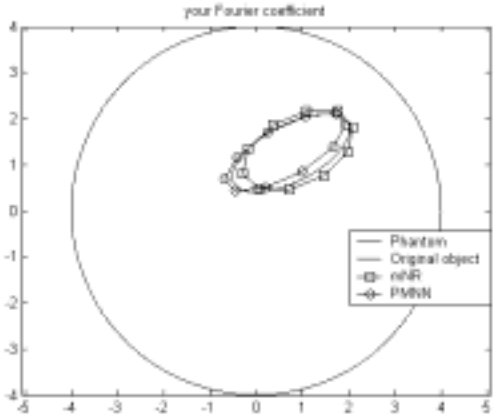

(b) γ = [0.75, 1.25, 0.20, 1.00 , 0.40, 0.75]

Fig. 5 Estimated boundary shape by PMNN and mNR with 3% noise

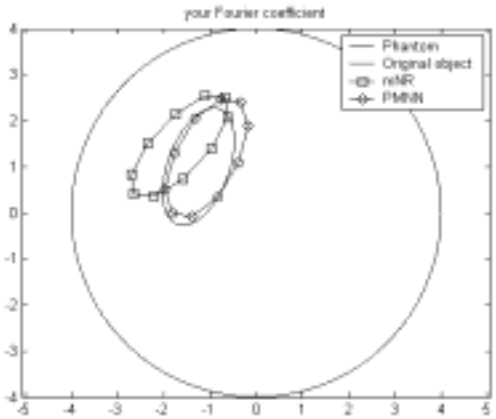

(a) γ = [-1.25, 0.75, 0.20, 1.00, 0.25, 1.25]

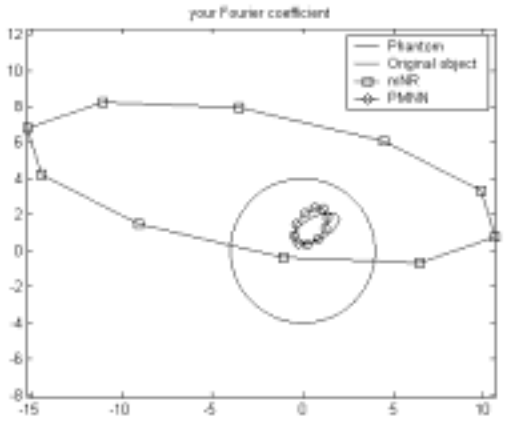

(b) γ = [0.75, 1.25, 0.20, 1.00 , 0.40, 0.75]
Fig. 6 Estimated boundary shape by PMNN and mNR with 3% noise

To analyze the reconstruction performance more qualitatively, we define the root mean square error (RMSE) as:

$$RMSE = \sqrt{\frac{(\gamma - \hat{\gamma})^T \cdot (\gamma - \hat{\gamma})}{\gamma^T \cdot \gamma}} \tag{17}$$

where $\hat{\gamma}$ represents estimated Fourier coefficient. The RMSE obtained from the assumed scenarios is summarized in Table 1.

Table 1 The RMSE of the two methods

RMSE		(a)	(b)
1% Noise	mNR	0.0704	0.0619
	PMNN	0.0426	0.1020
3% Noise	mNR	0.0739	0.1215
	PMNN	0.0736	0.1042
5% Noise	mNR	0.3399	7.3608
	PMNN	0.1375	0.2744

As we can be seen clearly in the Table 1, the proposed approach (PMNN) outperformed the mNR approach especially in the 3 and 5% noise level.

4. CONCLUSIONS

In this paper we have presented a parallel multi-layer neural network approach to the estimation of boundaries in the electrical impedance imaging of binary mixtures. The boundary shape is expressed in terms of the truncated Fourier coefficients, which are the unknowns to be determined with the over-determined boundary data of the injected currents and the measured voltages. The advantages of the proposed approach include high temporal resolution at the expense of long training time and robustness against the measurement noise.

For the verification of the performance on the parallel multi-layer neural network, we have conducted numerical simulations with single objects. In order to investigate the robustness against the noise in the measured boundary voltages we have considered various noise levels. Also, comparisons have been made with the results obtained by the conventional Newton type approach. It has been shown, especially, that the presented neural network can treat much higher noise level compared to the conventional Newton-type approach.

To improve the performance and availability of the proposed method, the optimization of the number of the hidden layers and the extension to the problems with multiple targets will be required.

ACKNOWLEDGMENTS

This work was supported by grant No. R01-2002-000-0040-0 (2003) from the Basic Research Program of the Korea Science & Engineering Foundation.

REFERENCES

[1] R. A. Williams and M. S. Beck (Eds.), Process Tomography – Principles, *Techniques and Applications*, Butterworth-Heinemann, Oxford, 1995.

[2] T. Dyakowski, L. F. C. Jeanmeure, and A. J. Jaworski, "Applications of electrical tomography for gas-solids and liquid-solids flows – a review," *Powder Technol*., vol. 112, pp. 174-192, 2000.

[3] K. H. Cho, S. Kim, and Y. J. Lee, "Impedance imaging of two-phase flow field with mesh grouping algorithm," *Nucl. Eng. Des*., vol. 204, pp. 57-67, 2001.

[4] M. C. Kim, S. Kim, and K. Y. Kim, "Enhancement of electrical impedance tomography images for the binary mixture system," in *2003 Proc of 3rd World Cong. Industrial Process Tomography*, pp. 677-682, Banff, Canada.

[5] M. Molinari, S. J. Cox, B. H. Blott, and G. J. Daniell, "Adaptive mesh refinement techniques for electrical impedance tomography," *Physiol. Meas*., vol. 22, pp. 91-96, 2001.

[6] D. K. Han and A. Prosperetti, "A shape decomposition technique in electrical impedance tomography," *J. Comput. Phys*., vol. 155, pp. 75-95, 1999.

[7] V. Kolehmainen, S. R. Arridge, W. R. B. Lionheart, M. Vauhkonen, and J. P. Kaipio, "Recovery of region boundaries of piecewise constant coefficients of elliptic PDE from boundary data," *Inverse Probl*. , vol. 15, pp. 1375-1391, 1999.

[8] H. J. Jeon, J. H. Kim, B. Y. Choi, M. C. Kim, K. Y. Kim, and S. Kim "Boundary Estimation in Two-Phase Flows with Electrical Impdance Imaging Technique," *Int. Comm. Heat and Mass Transfer*, accepted, 2004

[9] M. Vauhkonen, "Electrical impedance tomography and prior information," Ph.D. dissertation, Dept. Appl. Phys., Kuopio Univ., Kuopio, Finland, 1997.

[10] H. Y. Lee and K. I. Moon, *Fuzzy-Neural using MATLAB*. Seoul, Korea: Ajin Pub. Co., 1999, pp. 245-278. (in Korean)

[11] E. J. Woo, "Computational Complexity," *in Electrical Impedance Tomography*, J. G. Webster, Ed. Bristol: Adam Hilger, 1990, pp. 148-156.

[12] H. J. Jeon, B. Y. Choi, M. C. Kim, K. Y. Kim, S. Kim, "Phase Boundary Estimation in Two-Phase Flows with Electrical Impedance Imaging Technique," *Int. Comm. Heat Mass Transfer*, submitted for publication.